Probing the dynamical behavior of dark energy

Rong-Gen Cai,* Qiping Su,† and Hong-Bo Zhang‡

Key Laboratory of Frontiers in Theoretical Physics,

Institute of Theoretical Physics, Chinese Academy of Sciences,

P.O. Box 2735, Beijing 100190, China

Abstract

We investigate dynamical behavior of the equation of state of dark energy w_{de} by employing the linear-spline method in the region of low redshifts from observational data (SnIa, BAO, CMB and 12 $H(z)$ data). The redshift is binned and w_{de} is approximated by a linear expansion of redshift in each bin. We leave the divided points of redshift bins as free parameters of the model, if w_{de} changes its evolution direction in the considered region of redshift, the best-fitted values of divided points will represent the turning positions of w_{de}. These turning points are natural divided points of redshift bins, and w_{de} between two nearby divided points can be well approximated by a linear expansion of redshift. We only find two turning points of w_{de} in $z \in (0, 1.8)$ and one turning point in $z \in (0, 0.9)$, and $w_{de}(z)$ could be oscillating around $w = -1$. Moreover, we find that there is a 2σ deviation of w_{de} from -1 around $z = 0.9$ in both correlated and uncorrelated estimates.

PACS numbers: 98.80.Es, 95.36.+x, 98.80.-k

*Electronic address: cairg@itp.ac.cn

†Electronic address: sqp@itp.ac.cn

‡Electronic address: hbzhang@itp.ac.cn

I. INTRODUCTION

It has been more than ten years since our universe was found to be in accelerating expansion [1]. A dominated and uniformly distributed energy component of the universe, called dark energy (DE), should be responsible for the acceleration. Plenty of DE models have been proposed [2–6]. The simplest cosmological model is ΛCDM model, which contains a cosmological constant as dark energy. While ΛCDM model is still consistent well with all observational data, a lot of efforts have been made to find out whether DE is time-evolving or is just the cosmological constant. To do that, several parameterizations of equation of state (EoS) of DE have been proposed to fit with observational data, such as the ansatz $w_{de} = w_0 + w'z$ [7], the EoS expanded by redshift, and the CPL parametrization [8, 9] $w_{de} = w_0 + w_a z/(1+z)$, expanded by scale factor. Both of them contain two free parameters: w_0, the present value of EoS, and w' or w_a, represents the time evolution of EoS. Clearly, constraints of EoS obtained by using these parameterizations are model-dependent. Given an unreal assumption of EoS of DE, one may lead to wrong conclusions. Some model-independent methods have also proposed [10–13], such as the widely-used uncorrelated bandpower estimates (UBE) [11, 14], in which the redshift is binned and w_{de} is assumed as a constant in each redshift bin. Note that the UBE method just approximates the actual w_{de} by an averaged constant in each bin if DE is dynamical. If there are sufficient data, $w_{de}(z)$ can be accurately reconstructed. However, current data could only support a few bins, thus UBE is always used to test the deviation of w_{de} from the cosmological constant and used as a supplementary for the parameterizations of w_{de}. Note that the cubic-spline interpolation has been also proposed to study the binned $w_{de}(z)$ [15, 16]. However, no convincing evidence of dynamic DE has been found [15–17]. In addition, let us note that the ansatz, $w_{de} = w_0 + w'z$, of redshift expansion and CPL parametrization exclude the possibility of an oscillation EoS, if they are used to fit the whole expansion history of the universe. While the UBE method needs enough bins to reveal the real dynamical behavior of DE, the errors will get larger as the number of bins increases.

In this paper, we would like to probe the dynamical behavior of w_{de} by using the linear-spline method. We will approximate w_{de} in each redshift bin by a linear function $w = w_0 + w'z$, and require that $w_{de}(z)$ is continuous in the region under consideration. Since the most of data we used (e.g., SnIa data) are with low redshift, we will focus on the region of

low redshift, such as $z \in (0, 0.9)$ and $z \in (0, 1.8)$. In such regions, the width of redshift bins is small enough that the linear expansion could be a better approximation of $w_{de}(z)$ than a constant in each bin. When fitting with the observational data, we leave the divided positions of bins z_i as free parameters. Since the linear function is monotonic, the best-fitted z_i can represent the turning points of $w_{de}(z)$ if $w_{de}(z)$ is non-monotonic or is not linear enough in that region. Actually we do find some turning points of w_{de} from observational data, and the constructed $w_{de}(z)$ just turns its evolution direction at the best-fitted positions of z_i. In this way, we only need to divide redshift into a few bins, the turning points are natural divided points of redshift and w_{de} between two nearby points can be accurately reconstructed by linear expansion. Compared to the cubic-spline method, the linear-spline (LS) method can find the more accurate turning positions of w_{de} and reduce the errors due to less the number of bins. The LS method is also nearly model-independent, like the piecewise constant and cubic-spline method. Replacing the linear expansion by CPL parametrization in each bin, we have reached the almost same results.

For the current status of observational data, LS method may be more suitable to study w_{de} than the piecewise constant and the cubic spline method. If DE is dynamical or even oscillating, by using the LS method it should be more possible to find deviations from the cosmological constant, at the turning points the deviation from -1 should be more explicit. If DE is just the cosmological constant, it seems more confident if the best-fitted linear expansions construct an $w = -1$ line, while the oscillation of w_{de} around $w = -1$ could disappear by averaging with the piecewise constant method. Compared to the piecewise constant case, the only price we pay is that there is one more parameter in the LS method if the number of bins is the same in two cases. Compared to the cubic spline method, the form of $w_{de}(z)$ in each bin only depends on values of w_{de} at two boundaries, thus the parameters in $w_{de}(z)$ will not be heavily correlated. Furthermore, the cubic-spline method seems not suitable for finding the turning points of w_{de}. In all, the LS method could reconstruct w_{de} explicitly by using the least number of bins, and errors of the parameters from observational data will be small, compared to the case with more bins.

The paper is organized as follows. In section II we introduce in detail the method we will use and construct corresponding cosmological models. In section III, we show how to fit our model with 397 Constitution SnIa sample [18], BAO data from SDSS DR7 [19], CMB datapoints (R, l_a, z_*) from WMAP5 [20] and 12 Hubble evolution data [21, 22]. The fitting

results are presented in section IV. We give our conclusions and discussions in section V.

II. METHODOLOGY

To fit models with observational data, we need to know the form of Hubble function $H(z)$ (or $E(z) = H(z)/H_0$). In a flat FRW universe

$$E^2(z) = \frac{H^2(z)}{H_0^2} = \Omega_r^{(0)}(1+z)^4 + \Omega_b^{(0)}(1+z)^3 + \Omega_{dm}^{(0)}(1+z)^3 + \Omega_{de}^{(0)}F(z), \tag{1}$$

where $\Omega_r^{(0)}$, $\Omega_b^{(0)}$, $\Omega_{dm}^{(0)}$ and $\Omega_{de}^{(0)}$ are present values of the dimensionless energy density for radiations, baryons, dark matter and dark energy, respectively, and $\Omega_r^{(0)} + \Omega_b^{(0)} + \Omega_{dm}^{(0)} + \Omega_{de}^{(0)} = 1$. The energy densities of baryons and dark matter are always written together as $\Omega_b^{(0)}(1+z)^3 + \Omega_{dm}^{(0)}(1+z)^3 = \Omega_m^{(0)}(1+z)^3$. The radiation density is the sum of photons and relativistic neutrinos[20]:

$$\Omega_r^{(0)} = \Omega_\gamma^{(0)}(1 + 0.2271 N_n),$$

where N_n is the number of neutrino species and $\Omega_\gamma^{(0)} = 2.469 \times 10^{-5} h^{-2}$ for $T_{cmb} = 2.725K$ ($h = H_0/100\ km \cdot s^{-1}$). The evolving function $F(z)$ for DE depends on $w_{de}(z)$:

$$F(z) = e^{3\int_0^z \frac{1+w_{de}}{1+x}dx}. \tag{2}$$

For example,

$$F(z) = (1+z)^{3(1+w_0+w_a)} e^{-\frac{3w_a z}{1+z}},$$

for the CPL parametrization and $F(z) = 1$ for $w_{de} = -1$, respectively. Here we divide $z \in (0, \infty)$ into $m+1$ bins and assume $w_{de}(z)$ in the first m bins as

$$w_{de}(z_{n-1} < z \leq z_n) = w_{n-1} + w'_n \times (z - z_{n-1}) \ , \quad (1 \leq n \leq m) \tag{3}$$

and require $w_{de}(z)$ to be continuous at divided points:

$$w_n = w_{n-1} + w'_n \times (z_n - z_{n-1}) \ , \quad (1 \leq n \leq m-1) \tag{4}$$

Note that here " $'$ " does not represent a derivative, instead w'_n is just the slope of the linear expansion in the n^{th} bin. Thus the independent parameters are

$$w_0, w'_1, w'_2, ..., w'_n, ..., w'_m \tag{5}$$

where the total number of parameters is $1+m$ with $m \geq 1$. Alternatively, we can express the w_{de} as

$$w_{de}(z_{n-1} < z \leq z_n) = w(z_{n-1}) + \frac{w(z_n) - w(z_{n-1})}{z_n - z_{n-1}}(z - z_{n-1}) \ , \quad (1 \leq n \leq m) \tag{6}$$

Now the parameters become $w(z_n)$'s, which are values of w_{de} at the divided points and boundaries z_n $(0 \leq n \leq m)$. In this case we have

$$\begin{aligned} F(z_{n-1} < z \leq z_n) \ = \ & e^{3\{[w(z_{n-1})-w(0)]+\frac{w(z_n)-w(z_{n-1})}{z_n-z_{n-1}}(z-z_{n-1})\}} \left(\frac{1+z}{1+z_{n-1}}\right)^{3\frac{w(z_{n-1})(1+z_n)-w(z_n)(1+z_{n-1})}{z_n-z_{n-1}}} \\ & \times(1+z)^3 \prod_{i=1}^{n-1} \left(\frac{1+z_i}{1+z_{i-1}}\right)^{3\frac{w(z_{i-1})(1+z_i)-w(z_i)(1+z_{i-1})}{z_i-z_{i-1}}} \ , \quad (1 \leq n \leq m) \end{aligned} \tag{7}$$

where we have used $z_0 = 0$. For w_{de} in the last bin $z \in (z_m, \infty)$, we set it to be a constant w_L, and

$$F(z > z_m) = F(z_m)(1+z)^{3(1+w_L)} \tag{8}$$

Now the formula for $H(z)$ is ready.

There is one more thing to be mentioned: once we have fitted our model with the data introduced in the next section, the errors of $w(z_i)$ are correlated. Though there are different interpretations for errors of correlated and uncorrelated parameters [23], we will also show results of the uncorrelated parameters. The uncorrelated technique we adopt from [11] is as follows.

1. Get the covariance matrix

$$C = \langle WW^T \rangle - \langle W \rangle \langle W^T \rangle \tag{9}$$

where W is the vector of $w(z_i)$. The Fisher matrix F is defined by $F = C^{-1}$.

2. Diagonalize the Fisher matrix by an orthogonal matrix O

$$F = O^T \Lambda O, \tag{10}$$

where Λ is diagonal.

3. Define a new matrix U as

$$U = O^T \Lambda^{1/2} O, \tag{11}$$

and normalize U so that the sum of its each row is equal to 1.

4. Define new parameters q_i by $q = UW$, where q_i are components of the vector q.

Clearly for the case of $w(z) = -1$ (i.e., the cosmological constant case), we will have $q_i = -1$. The covariance of new parameters is

$$\langle (q_i - \langle q_i \rangle)(q_j - \langle q_j \rangle) \rangle = \frac{\delta_{ij}}{\sum_a (F^{1/2})_{ia} \sum_b (F^{1/2})_{jb}}. \tag{12}$$

In this way the errors of the new parameters q_i are uncorrelated.

The uncorrelated parameters q_i are linear combinations of $w(z_i)$, and the coefficients are just row elements of U. The transformation matrix U constructed in this method ensures that most of the coefficients are positive. So most of coefficients are in $(0, 1)$. In this way, the original correlated parameters are weighted averaged, which leads to the uncorrelated parameters q_i. As a result, if w_{de} is of the quintom form, the uncorrelated w_{de} always looks more consistent with the cosmological constant than the correlated one.

III. SETS OF OBSERVATIONAL DATA

We will fit our model by employing some observational data including SnIa, BAO, CMB and Hubble evolution data. The data for SnIa are the 397 Constitution sample [18]. χ^2_{sn} for SnIa is obtained by comparing theoretical distance modulus $\mu_{th}(z) = 5\log_{10}[(1+z)\int_0^z dx/E(x)] + \mu_0$ ($\mu_0 = 42.384 - 5\log_{10} h$) with observed μ_{ob} of supernovae:

$$\chi^2_{sn} = \sum_i^{397} \frac{[\mu_{th}(z_i) - \mu_{ob}(z_i)]^2}{\sigma^2(z_i)} \tag{13}$$

To reduce the effect of μ_o, we expand χ^2_{sn} with respect to μ_0 [24]:

$$\chi^2_{sn} = A + 2B\mu_0 + C\mu_0^2 \tag{14}$$

where

$$\begin{aligned} A &= \sum_i \frac{[\mu_{th}(z_i; \mu_0 = 0) - \mu_{ob}(z_i)]^2}{\sigma^2(z_i)} , \\ B &= \sum_i \frac{\mu_{th}(z_i; \mu_0 = 0) - \mu_{ob}(z_i)}{\sigma^2(z_i)}, \; C = \sum_i \frac{1}{\sigma^2(z_i)} \end{aligned} \tag{15}$$

Eq. (14) has a minimum as

$$\widetilde{\chi}^2_{sn} = \chi^2_{sn,min} = A - B^2/C$$

which is independent of μ_0. We will adopt $\widetilde{\chi}^2_{sn}$ as the chi-square between theoretical model and SnIa data.

The second is the Baryon Acoustic Oscillations (BAO) data from SDSS DR7 [19], the datapoints we use are

$$\frac{r_s(z_d)}{D_V(0.275)} = 0.1390 \pm 0.0037 \tag{16}$$

and

$$\frac{D_V(0.35)}{D_V(0.2)} = 1.736 \pm 0.065 \tag{17}$$

where $r_s(z_d)$ is the comoving sound horizon at the baryon drag epoch [25], and

$$D_V(z) = \left[\left(\int_0^z \frac{dx}{H(x)} \right)^2 \frac{z}{H(z)} \right]^{1/3} \tag{18}$$

encodes the visual distortion of a spherical object due to the non Euclidianity of a FRW space-time.

The CMB datapoints we will use are (R, l_a, z_*) from WMAP5 [20]. z_* is the redshift of recombination [26], R is the scaled distance to recombination

$$R = \sqrt{\Omega_m^{(0)}} \int_0^{z_*} \frac{dz}{E(z)}, \tag{19}$$

and l_a is the angular scale of the sound horizon at recombination

$$l_a = \pi \frac{r(a_*)}{r_s(a_*)}, \tag{20}$$

where $r(z) = \int_0^z dx/H(x)$ is the comoving distance and $r_s(a_*)$ is the comoving sound horizon at recombination

$$r_s(a_*) = \int_0^{a_*} \frac{c_s(a)}{a^2 H(a)} da, \quad a_* = \frac{1}{1+z_*} \tag{21}$$

where the sound speed $c_s(a) = 1/\sqrt{3(1+\overline{R}_b a)}$ and $\overline{R}_b = 3\Omega_b^{(0)}/4\Omega_\gamma^{(0)}$ is the photon-baryon energy density ratio.

The χ^2 of the CMB data is constructed as:

$$\chi^2_{cmb} = X^T C_M^{-1} X \tag{22}$$

where

$$X = \begin{pmatrix} l_a - 302.1 \\ R - 1.71 \\ z_* - 1090.04 \end{pmatrix} \tag{23}$$

and the inverse covariance matrix

$$C_M^{-1} = \begin{pmatrix} 1.8 & 27.968 & -1.103 \\ 27.968 & 5667.577 & -92.263 \\ -1.103 & -92.263 & 2.923 \end{pmatrix} \tag{24}$$

The fourth set of observational data is 12 Hubble evolution data from [21] and [22], its χ^2_H is defined as

$$\chi^2_H = \sum_{i=1}^{12} \frac{[H(z_i) - H_{ob}(z_i)]^2}{\sigma_i^2}. \tag{25}$$

Note that redshifts of these data fall in the region $z \in (0, 1.75)$.

IV. FITTING RESULTS

A. Model I

At first, we divide the whole region of redshift into 4 bins (i.e., $m = 3$), the divided points and boundaries are $(0, z_1, z_2, 1.8, \infty)$, where z_1 and z_2 are left as free parameters of the model,

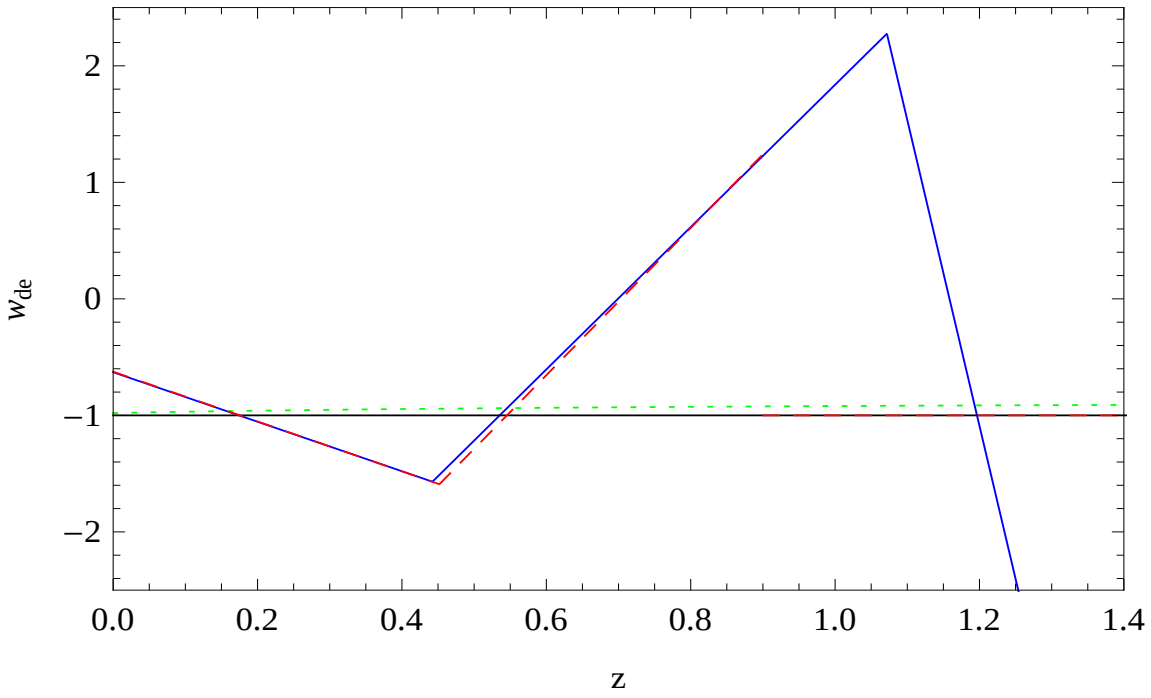

FIG. 1: The best-fitted w_{de} for Model I (blue, solid), Model II (red, dashed) and the CPL model (green, dotted), the black line is for $w = -1$.

and $0 < z_1 < z_2 < 1.8$. In the fourth bin we set $w_L = -1$. It means that we divide the region with $z \in (0, 1.8)$ into 3 bins and seek for two possible turning points of $w_{de}(z)$ in this region. The reconstructed w_{de} of the best-fitted model is shown in Fig. 1, which indicates that there exist (at least) two turning points of w_{de} in $z \in (0, 1.8)$ and the best-fitted values $z_1 = 0.44$ and $z_2 = 1.07$. Here $\chi^2_{min} = 467.410$ for the best-fitted parameters, roughly speaking it is a good improvement, compared with the corresponding $\chi^2_{min} = 478.407$ for the best-fitted CPL model and $\chi^2_{min} = 479.092$ for the ΛCDM model. It implies that the data favor w_{de} to turn its evolution direction around $z = 0.44$ and $z = 1.07$, respectively. Of course this result also implies that there exists the possibility with an oscillating EoS. Note that the error bar of w_{de} in the third bin is larger than those in the first two bins because the data points in that bin are much less.

We have also divided the region of $z \in (0, 1.8)$ into 4 bins, but found no more turning points of w_{de} in this region and there is almost no improvement of χ^2_{min} compared to the case of 3 bins.

TABLE I: The best-fitted parameters for Model I.

parameters	h	$\Omega_b^{(0)}$	$\Omega_m^{(0)}$	z_1	z_2	$w(0)$	$w(z_1)$	$w(z_2)$	$w(1.8)$	w_L
best-fitted values	0.688	0.049	0.279	0.44	1.07	-0.63	-1.57	2.28	-16.84	{-1}

B. Model II

As data points with $z > 1$ are rather less than those with $z < 1$, to see clearly the evolution behavior of EoS in the region of low redshift, we now focus on the region with $z \in (0, 0.9)$, avoiding the possible turning point around $z = 1$, and set the divided points as: $(0, z_1, 0.9, \infty)$, i.e.,

$$w_{de}(z) = \begin{cases} w(0) + \frac{w(z_1)-w(0)}{z_1} z \ , & 0 < z \leq z_1 \\ w(z_1) + \frac{w(0.9)-w(z_1)}{0.9-z_1}(z - z_1) \ , & z_1 < z \leq 0.9 \\ -1 \ , & 0.9 < z < \infty \end{cases} \tag{26}$$

In this case, we obtain the best-fitted tuning point $z_1 = 0.45$, and the best-fitted $w_{de}(z)$ is shown in Fig. 1 (the red, dashed line) which almost coincides with the best-fitted $w_{de}(z)$ of Model I in $z \in (0, 0.9)$. This indicates that the data favor $w_{de}(z)$ to turn its evolution

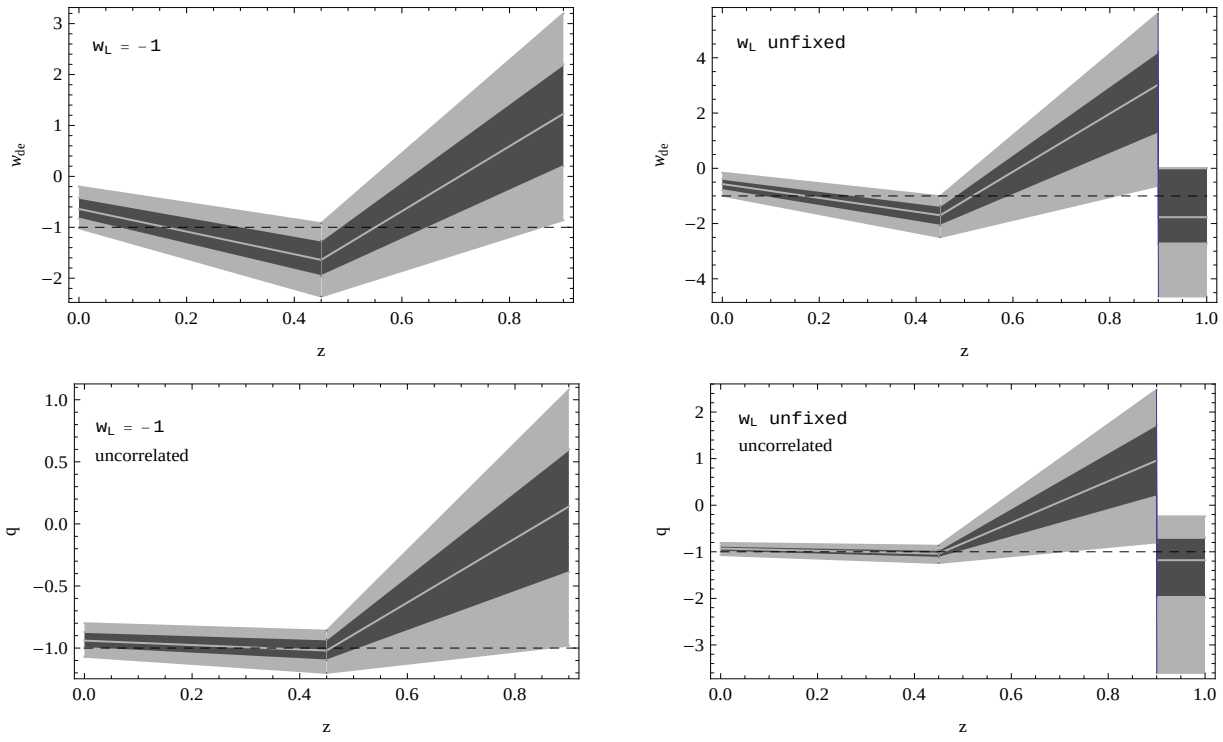

FIG. 2: 1σ and 2σ errors of w_{de} in Model II. Left panels are for the model with $w_L = -1$ and right panels are with w_L unfixed, top panels are for correlated parameters in $w_{de}(z)$ and the bottom panels are for uncorrelated ones.

direction around $z = 0.45$, and favor an EoS with crossing the cosmological constant ($w = -1$) [27]. Then we obtain 1σ and 2σ errors of parameters (shown in Fig. 2) by using the MCMC method. Here we have fixed $z_1 = 0.45$ in the process to obtain the errors of the parameters.

We see from the upleft panel of Fig. 2 that there are deviations of w_{de} from -1 around $z = 0$ and $z = 0.45$ beyond 1σ, and around $z = 0.9$ the deviation is beyond 2σ. We uncorrelate the parameters in $w_{de}(z)$ by using the technique introduced in section II. The uncorrelated errors are shown in the bottom left panel of Fig. 2. In that case, there are no more explicit deviations from -1 around $z = 0$ and $z = 0.45$, however, there is still a 2σ deviation from -1 around $z = 0.9$.

One may suspect that the explicit derivations are caused due to the fact that we have fixed the value of w_{de} as $w_L = -1$ in the third bin. To check this, we consider the case with an unfixed w_L. Two right panels of Fig. 2 show the correlated and uncorrelated results for the case with an unfixed w_L. We see that in this case, there is even larger deviation

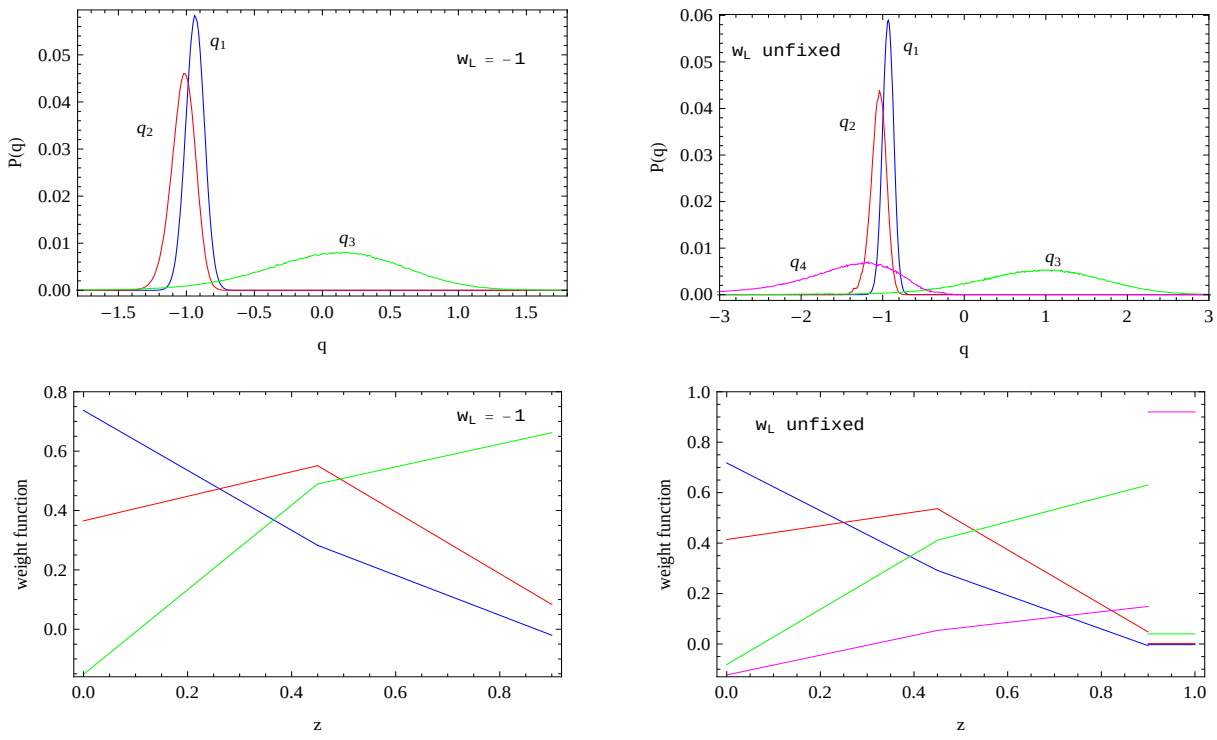

FIG. 3: Likelihoods and weight functions of uncorrelated parameters q_i and corresponding weight functions. The left panels are for the model with $w_L = -1$ and the right panels are for that with w_L unfixed.

from -1 around $z = 0.9$. We have also used the CPL parametrization to replace the linear expansion in each bin, and found that the errors are almost the same as those in the case of the linear expansion and there is still a deviation of w_{de} from -1 around $z = 0.9$. We have more discussions on this in the last section. In Fig. 3 we plot the likelihoods and weight functions of the uncorrelated parameters q_i. It is shown that the parameters of w_{de} are not heavily correlated.

TABLE II: The best-fitted parameters and 2σ errors for Model II with w_L fixed to -1 or unfixed. ML is for "Maximum Likelihood", and the value in {} means this parameter has been fixed.

parameters	h	$\Omega_b^{(0)}$	$\Omega_m^{(0)}$	z_1	$w(0)$	$w(z_1)$	$w(0.9)$	w_L
best-fitted values	0.684	0.050	0.282	0.45	-0.63	-1.59	1.24	{-1}
ML and 2σ errors	$0.684^{+0.025}_{-0.026}$	$0.050^{+0.004}_{-0.003}$	$0.286^{+0.03}_{-0.03}$	{0.45}	$-0.64^{+0.44}_{-0.38}$	$-1.64^{+0.72}_{-0.72}$	$1.23^{+1.97}_{-2.09}$	{-1}
best-fitted values	0.687	0.049	0.280	{0.45}	-0.59	-1.69	2.54	-1.72
ML and 2σ errors	$0.687^{+0.027}_{-0.026}$	$0.049^{+0.004}_{-0.004}$	$0.285^{+0.033}_{-0.030}$	{0.45}	$-0.57^{+0.41}_{-0.42}$	$-1.70^{+0.69}_{-0.79}$	$3.03^{+2.58}_{-3.66}$	$-1.77^{+1.78}_{-2.87}$

We have also divided $z \in (0, 0.9)$ into three bins, to see whether there exist two turning points of w_{de} in this region. We found that with the additional 2 parameters (z_2 and $w(z_2)$), there is almost no improvement of χ^2_{min}, compared to the 2 bins case (Model II). This indicates that there is no more turning points and $w_{de}(z)$ can be well approximated by just two linear expansions in the region $z \in (0, 0.9)$. Of course, there is another possibility that the current data are not enough to find out more turning points.

V. CONCLUSIONS AND DISCUSSIONS

In this paper we have investigated the dynamical behavior of the EoS of DE in the region of low redshift in a nearly model-independent way. The redshift in that region is binned and w_{de} in each bin is approximated by a linear expansion of redshift z, and in the large redshift region we set w_{de} to be a constant w_L. While fitting the model with some observational data which include SnIa, BAO, CMB and Hubble evolution data, we leave the divided points of bins as free parameters. If the evolution of w_{de} is not monotonous, or is not linear enough in the region under consideration, the best-fitted divided points will represent the turning points, where w_{de} changes its evolution direction significantly. In this way we can explicitly reconstruct w_{de} by using a few bins, and the errors of parameters from observational data will be small due to the small number of bins. First we have tried to find the turning points within the region of redshift $z \in (0, 1.8)$, and set $w_L = -1$ in the region $z \in (1.8, \infty)$ (Model I). Our results show that the data favor two turning points of w_{de} in $z \in (0, 1.8)$, and w_{de} may have an oscillation form [28]. Our results are consistent with those by the UBE method in [29].

Since the main data points are in $z \in (0, 1)$ and our result in Model I shows there may be a turning point around $z \sim 1$, to see clearly the dynamical behavior of EoS in that region, we have focused on the region $z \in (0, 0.9)$ in Model II. We have found one turning point only in $z \in (0, 0.9)$, the reconstructed w_{de} in the best-fitted model is almost the same as that reconstructed in Model I in $z \in (0, 0.9)$. We have also obtained the errors of w_{de} at 1σ and 2σ in $z \in (0, 0.9)$. In both correlated and uncorrelated estimates with a fixed $w_L = -1$ or an unfixed constant w_L, we found that there is a 2σ deviation of w_{de} from -1 around $z = 0.9$.

It is interesting to see whether the deviation of EoS from -1 around $z = 0.9$ is physical,

or is caused by some unknown technical causes in fitting. If it is physical, it then clearly shows that DE is dynamical. But in UBE of w_{de} there seems no such distinct deviation around $z = 0.9$, it may be due to the difference between the discontinuity of w_{de} in the piecewise constant case and the continuity in LS case [30]. In [16], where the cubic-spline method is used, there is also no such an explicit deviation around $z = 0.9$, but it is likely due to its set of EoS in the last bin $w_L = w(1)$: to fit well with the data of $z > 1$, $w(1)$ should be much minus, which would suppress the reconstructed w_{de} around $z = 1$. Of course, it is also possible that such a big deviation around $z = 0.9$ is due to the non-smoothness of w_{de} at the divided points in our LS method. In the LS method, w_{de} is continuous, but not smooth at the divided points, i.e., its derivative is not continuous in these points. In fact, the w_{de} in LS method can be smoothed at the divided points, such as:

$$w_{de}(z) = w_0 + \sum_{i=1}^{m} \frac{w'_i - w'_{i-1}}{2}(z + \Delta \ln \frac{\cosh(\frac{z-z_{i-1}}{\Delta})}{\cosh(z_{i-1}/\Delta)}), \tag{27}$$

where w'_i is the slope of linear expansion in the i^{th} bin ($i \geq 1$ and $w'_0 = 0$), and Δ is related to the smoothed extent at the divided points. With this parameterization, one can still find out the turning positions of w_{de} that are favored by observational data, and perturbations of DE can be calculated.

Furthermore our results are also dependent on the data set we have used [31]. For example, though there is still a 2σ deviation at $z = 0.9$ by using the widely-used data set SnIa + CMB-shift R + BAO parameter A[32], now the best-fitted turning point in $z \in (0, 0.9)$ changes to $z = 0.39$. Whatever, from the observational data we have used, a big deviation of w_{de} from -1 around $z = 0.9$ is found. Unlike the deviations around $z = 0$ and $z = 0.45$, this deviation around $z = 0.9$ does not to be reduced in the uncorrelated estimate. At least, our result shows that if DE is dynamic it is more possible to find the deviation of w_{de} from -1 around this position of redshift.

If the EoS of DE is indeed of an oscillating behavior around -1, it is then not surprised that the cosmological constant always fits well with observational data because the oscillating behavior could be smeared in the luminosity distance. However, if the oscillation region of w_{de} is wide enough (like the case of our best-fitted w_{de} in Model I), DE may be distinguished confidently from the cosmological constant by more precise astronomical observations in the next generation. In addition, let us mention that an oscillating behavior of w_{de} is also possibly due to some systematic errors in observational data, or due to some interactions

between DE and dark matter [33].

Acknowledgments

RGC thanks Y.G. Gong and B. Wang for some relevant discussions. This work was partially supported by NNSF of China (No. 10821504 and No. 10975168) and the National Basic Research Program of China under grant 2010CB833000.

---

[1] A. G. Riess *et al.* [Supernova Search Team Collaboration], Astron. J. **116**, 1009 (1998) [arXiv:astro-ph/9805201]; S. Perlmutter *et al.* [Supernova Cosmology Project Collaboration], Astrophys. J. **517**, 565 (1999) [arXiv:astro-ph/9812133].

[2] E. J. Copeland, M. Sami and S. Tsujikawa, Int. J. Mod. Phys. D **15**, 1753 (2006) [arXiv:hep-th/0603057].

[3] R. R. Caldwell and P. J. Steinhardt, Phys. Rev. D **57**, 6057 (1998) [arXiv:astro-ph/9710062].

[4] P. J. Steinhardt, L. M. Wang and I. Zlatev, Phys. Rev. D **59**, 123504 (1999) [arXiv:astro-ph/9812313].

[5] S. Capozziello, S. Carloni and A. Troisi, Recent Res. Dev. Astron. Astrophys. **1**, 625 (2003) [arXiv:astro-ph/0303041].

[6] M. Li, Phys. Lett. B **603**, 1 (2004) [arXiv:hep-th/0403127]; R. G. Cai, Phys. Lett. B **657**, 228 (2007) [arXiv:0707.4049 [hep-th]]; H. Wei and R. G. Cai, Phys. Lett. B **660**, 113 (2008) [arXiv:0708.0884 [astro-ph]]. B. Feng, X. L. Wang and X. M. Zhang, Phys. Lett. B **607**, 35 (2005) [arXiv:astro-ph/0404224]; C. Gao, X. Chen and Y. G. Shen, Phys. Rev. D **79**, 043511 (2009) [arXiv:0712.1394 [astro-ph]].

[7] D. Huterer and M. S. Turner, Phys. Rev. D **64**, 123527 (2001) [arXiv:astro-ph/0012510]; D. Huterer and M. S. Turner, Phys. Rev. D **60**, 081301 (1999) [arXiv:astro-ph/9808133]; J. Weller and A. J. Albrecht, Phys. Rev. Lett. **86**, 1939 (2001) [arXiv:astro-ph/0008314].

[8] M. Chevallier and D. Polarski, Int. J. Mod. Phys. D **10**, 213 (2001) [arXiv:gr-qc/0009008].

[9] E. V. Linder, Phys. Rev. Lett. **90**, 091301 (2003) [arXiv:astro-ph/0208512].

[10] D. Huterer and G. Starkman, Phys. Rev. Lett. **90**, 031301 (2003) [arXiv:astro-ph/0207517].

[11] D. Huterer and A. Cooray, Phys. Rev. D **71**, 023506 (2005) [arXiv:astro-ph/0404062].

[12] A. Hojjati, L. Pogosian and G. B. Zhao, arXiv:0912.4843 [astro-ph.CO].

[13] Y. Wang, Phys. Rev. D **80**, 123525 (2009) [arXiv:0910.2492 [astro-ph.CO]].

[14] S. Sullivan, A. Cooray and D. E. Holz, JCAP **0709**, 004 (2007) [arXiv:0706.3730 [astro-ph]].

[15] G. B. Zhao, D. Huterer and X. Zhang, Phys. Rev. D **77**, 121302 (2008) [arXiv:0712.2277 [astro-ph]].

[16] P. Serra, A. Cooray, D. E. Holz, A. Melchiorri, S. Pandolfi and D. Sarkar, arXiv:0908.3186 [astro-ph.CO].

[17] Y. Gong, R. G. Cai, Y. Chen and Z. H. Zhu, arXiv:0909.0596 [astro-ph.CO].

[18] M. Hicken *et al.*, Astrophys. J. **700**, 331 (2009) [arXiv:0901.4787 [astro-ph.CO]].

[19] W. J. Percival *et al.*, arXiv:0907.1660 [astro-ph.CO].

[20] E. Komatsu *et al.* [WMAP Collaboration], Astrophys. J. Suppl. **180**, 330 (2009) [arXiv:0803.0547 [astro-ph]].

[21] J. Simon, L. Verde and R. Jimenez, Phys. Rev. D **71**, 123001 (2005) [arXiv:astro-ph/0412269].

[22] E. Gaztanaga, A. Cabre and L. Hui, arXiv:0807.3551 [astro-ph].

[23] R. de Putter and E. V. Linder, Astropart. Phys. **29**, 424 (2008) [arXiv:0710.0373 [astro-ph]].

[24] S. Nesseris and L. Perivolaropoulos, Phys. Rev. D **72**, 123519 (2005) [arXiv:astro-ph/0511040].

[25] D. J. Eisenstein and W. Hu, Astrophys. J. **496**, 605 (1998) [arXiv:astro-ph/9709112].

[26] W. Hu and N. Sugiyama, Astrophys. J. **471**, 542 (1996) [arXiv:astro-ph/9510117].

[27] H. Zhang, arXiv:0909.3013 [astro-ph.CO].

[28] R. Lazkoz, S. Nesseris and L. Perivolaropoulos, JCAP **0511**, 010 (2005) [arXiv:astro-ph/0503230]; M. X. Luo and Q. P. Su, Phys. Lett. B **626**, 7 (2005) [arXiv:astro-ph/0506093].

[29] Q. G. Huang, M. Li, X. D. Li and S. Wang, Phys. Rev. D **80**, 083515 (2009) [arXiv:0905.0797 [astro-ph.CO]]; G. B. Zhao and X. Zhang, arXiv:0908.1568 [astro-ph.CO]; S. Qi, T. Lu and F. Y. Wang, arXiv:0904.2832 [astro-ph.CO].

[30] In preparing.

[31] J. C. B. Sanchez, S. Nesseris and L. Perivolaropoulos, JCAP **0911**, 029 (2009) [arXiv:0908.2636 [astro-ph.CO]]; H. Wei, arXiv:0906.0828 [astro-ph.CO]; Y. Gong, B. Wang and R. G. Cai, arXiv:1001.0807 [astro-ph.CO].

[32] D. J. Eisenstein *et al.* [SDSS Collaboration], Astrophys. J. **633**, 560 (2005) [arXiv:astro-ph/0501171].

[33] J. H. He, B. Wang and P. Zhang, Phys. Rev. D **80**, 063530 (2009) [arXiv:0906.0677 [gr-qc]]; R. G. Cai and Q. Su, arXiv:0912.1943 [astro-ph.CO]; C. Feng, B. Wang, E. Abdalla and R. K. Su, Phys. Lett. B **665**, 111 (2008) [arXiv:0804.0110 [astro-ph]]; H. H. Xiong, Y. F. Cai, T. Qiu, Y. S. Piao and X. Zhang, Phys. Lett. B **666**, 212 (2008) [arXiv:0805.0413 [astro-ph]].